

Rare examples of diphenoxido-bridged trinuclear $\text{Ni}^{\text{II}}\text{Fe}^{\text{III}}$ complexes with a reduced salen type Schiff base ligand: Structures and magnetic properties

Alokesh Hazari ^{a,b}, Carlos J. Gómez-García ^c, Michael G.B. Drew ^d, Ashutosh Ghosh ^{a,*}

^a Department of Chemistry, University College of Science, University of Calcutta, 92, APC Road, Kolkata 700009, India

^b Department of Chemistry, Government General Degree College Singur, Jalaghata, Hooghly, 712 409, India

^c Instituto de Ciencia Molecular (ICMol), Dpt. Química Inorgánica, Universidad de Valencia, C/Catedrático José Beltrán, 2, 46980 Paterna, Valencia, Spain

^d School of Chemistry, The University of Reading, P.O. Box 224, Whiteknights, Reading RG6 6AD, United Kingdom



ARTICLE INFO

Article history:

Received 8 July 2017

Accepted 11 September 2017

Available online 21 September 2017

Keywords:

Nickel(II)

Iron(III)

$\mu_{1,3}$ -azido bridging

Reduced Schiff base

Magnetic properties

ABSTRACT

Three new trinuclear hetero-metallic complexes, $[(\text{NiL}^{\text{R}})_2\text{Fe}(\text{N}_3)_3]$ (**1**), $[(\text{NiL}^{\text{R}}(\text{H}_2\text{O}))_2\text{Fe}(\text{C}_6\text{H}_5\text{CH}_2\text{CO}_2)_2]\cdot(\text{HSO}_4)$ (**2**) and $[(\text{NiL}^{\text{R}}(\text{H}_2\text{O}))_2\text{Fe}(\text{C}_6\text{H}_5\text{CO}_2)_2]\cdot(\text{HSO}_4)\cdot(\text{H}_2\text{O})\cdot(\text{CH}_2\text{Cl}_2)$ (**3**) have been synthesized using $[\text{NiL}^{\text{R}}]$ as a “metalloligand” (where $\text{H}_2\text{L}^{\text{R}} = \text{N,N}'\text{-bis}(2\text{-hydroxybenzyl})\text{-}1,3\text{-propanediamine}$). All complexes have been characterized by elemental analysis, spectroscopic methods, single crystal XRD and magnetic study. In the angular trinuclear units of **1**, the two terminals $[\text{NiL}^{\text{R}}]$ coordinate through double phenoxido bridges to the central Fe^{III} ion which is penta-coordinated having terminally coordinated azide ion. The two terminal Ni^{II} centers are connected to each other and also to neighbouring units through $\mu_{1,3}$ -azido bridges to form an alternating chain. On the other hand, complexes, **2** and **3** are linear discrete trinuclear species $[\text{Ni}^{\text{II}}\text{-}\text{Fe}^{\text{III}}\text{-}\text{Ni}^{\text{II}}]$ in which two terminal octahedral $[\text{NiL}^{\text{R}}]$ units coordinate to the central octahedral Fe^{III} ion, located on a crystallographic centre of symmetry, through a μ_2 -phenoxido oxygen atom and a bridging carboxylato ion. Variable temperature magnetic susceptibility measurements show the presence of antiferromagnetic exchange interactions in **1** mediated through the phenoxido bridges ($J_1 = -33.2 \text{ cm}^{-1}$), and $\mu_{1,3}\text{-N}_3$ single bridges ($J_2 = -19.9 \text{ cm}^{-1}$ and $J_3 = -16.7 \text{ cm}^{-1}$). On the other hand, compounds **2** and **3** show ferromagnetic coupling interactions mediated through the double phenoxido bridges with J values of $+4.9$ and $+3.0 \text{ cm}^{-1}$ for **2** and **3**, respectively.

© 2017 Elsevier Ltd. All rights reserved.

1. Introduction

The design and synthesis of polynuclear metal complexes have become a very popular research topic in the last decades not only for their attractive structures but also for their diverse applications such as optical materials, magnetic materials and catalysts for organic reactions [1–4]. The knowledge of the magnetic properties and the factors governing them in polynuclear complexes is a key factor for the design and development of polynuclear complexes with interesting and pre-defined magnetic properties in order to prepare SMM or magnetic MOFs with interesting applications in magnetic sensors, memory devices, low density magnets, separation of magnetic molecules etc.

The majority of these complexes have been synthesized with first row transition metals (3d) [5], although complexes of other

transition metals (4d,5d) [6,7] as well as rare earth metals (4f, 5f) [8,9] are also well known. An important subgroup of the complexes is formed by the hetero-metallic complexes, where almost all possible combinations of transition metals [10] and/or rare earth metals [11,12] are known. For the designed synthesis of such complexes the choice of ligands is the most important issue. The salen type di-Schiff base ligands offer a very straight forward way for such synthesis as the two oxygen atoms of their neutral mononuclear complexes of divalent metal ions can coordinate easily to another metal ion to produce hetero-polynuclear complexes [13,14]. Among the divalent 3d transition metal ions, complexes of Cu(II) [15] and Ni(II) [16] are the most stable and therefore have been widely exploited for this purpose. Recently, we found that complexes of reduced Schiff bases can also be used as “metalloligands” as efficiently as their unreduced analogues [17]. Moreover, they can bring about interesting variations in the structures due to increased flexibility of the ligand backbone and potential formation of hydrogen bonds [18]. A recent search in

* Corresponding author.

E-mail address: ghosh_59@yahoo.com (A. Ghosh).

the CCDC database for hetero-metallic complexes where Schiff base complexes of Cu(II) or Ni(II) are connected to any transition metal atom through the phenoxido bridge locates several dinuclear [19] and trinuclear, [20] and a few polynuclear [21] species. Among these, the trinuclear MCu_2 [22] or MNi_2 [23] (where M = any transition metal atom other than Cu or Ni) species are the most abundant, especially with salen type Schiff bases. However, when iron is the hetero-atom (M = Fe), only one trinuclear [24] and one trinuclear-based chain structure [25] with Cu(II) but no trinuclear phenoxido bridged Ni₂Fe complex with salen type Schiff base are reported till date. Although there is one similar trinuclear Ni₂Fe complex but that is derived from a tripodal hexadentate Schiff base ligand [26].

The phenoxido bridge is well known for transmitting ferro- or anti-ferromagnetic exchange between paramagnetic metal centres depending mostly on the bridging angle [23a,27]. The crossover angles where ferromagnetic coupling changes to anti-ferromagnetic have been established experimentally and theoretically for the homo-metallic complexes by various groups [28]. However, for hetero-metallic complexes such studies are rare, presumably due to the paucity of synthesized complexes. If we consider phenoxido bridged Ni^{II}/Fe^{III} complexes including all kinds of ligands, there are a total of 13 complexes [29–31], 12 of which have been magnetically characterized [26,29–30]. Among these twelve complexes, eleven are dimers [29,30] and the remaining one is the previously mentioned trimer [26]. In the dinuclear complexes, the Ni—O(phenoxido)—Fe bridging angles are found to vary between 116.43° and 88.67° and the crossover angle has been estimated to be 95.51° [29b]. The magnetic properties of the only trinuclear complex [26] are rather surprising as it showed anti-ferromagnetic coupling for a bridging angle of 86.23°, well below the crossover angle. This surprising result and the lack of other examples of this kind of polynuclear complexes prompted us to synthesize some diphenoxido-bridged trinuclear Ni^{II}/Fe^{III} complexes in order to study their magnetic coupling.

Here, we present the syntheses, X-ray crystal structures, and magnetic properties of three new complexes formulated as $[(\text{NiL}^R)_2\text{Fe}(\text{N}_3)_3]$ (**1**), $[(\text{NiL}^R(\text{H}_2\text{O}))_2\text{Fe}(\text{C}_6\text{H}_5\text{CH}_2\text{CO}_2)_2]\cdot(\text{HSO}_4)$ (**2**) and $[(\text{NiL}^R(\text{H}_2\text{O}))_2\text{Fe}(\text{C}_6\text{H}_5\text{CO}_2)_2]\cdot(\text{HSO}_4)\cdot(\text{H}_2\text{O})\cdot(\text{CH}_2\text{Cl}_2)$ (**3**) (where $\text{H}_2\text{L}^R = \text{N,N}'\text{-bis}(2\text{-hydroxybenzyl})\text{-}1,3\text{-propanediamine}$). These complexes are the first examples of double phenoxido bridged trinuclear Ni₂Fe units derived from salen type N₂O₂ donor reduced Schiff base ligands. Magnetic measurements reveal antiferromagnetic interactions in complex **1** and ferromagnetic interactions in complexes **2** and **3**, which have been well explained considering their respective structural parameters.

2. Experimental

2.1. Starting materials

Salicylaldehyde, 1,3-propanediamine and sodium borohydride were purchased from Lancaster and were of reagent grade. They were used without further purification.

Caution! Azide salts and Perchlorate salts of metal complexes with organic ligands are potentially explosive. Only a small amount of material should be prepared and it should be handled with care.

2.2. Synthesis of the reduced Schiff base ligand, $\text{N,N}'\text{-bis}(2\text{-hydroxybenzyl})\text{-}1,3\text{-propanediamine}$ (H_2L^R) and “metalloligand”, $[\text{NiL}^R]$

The di-Schiff base ligand from 1,3-propanediamine and salicylaldehyde was synthesized by a reported method [32]: 5 mmol

of 1,3-propanediamine (0.42 mL) was mixed with 10 mmol of the salicylaldehyde (1.04 mL) in methanol (25 mL). The resulting solution was refluxed for ca. 2 h and allowed to cool. Then 25 mL (5 mmol) of this yellow methanolic ligand solution (H_2L) was cooled to 0 °C, and sodium borohydride (456 mg, 12 mmol) was added to this methanol solution with stirring. After completion of addition, the resulting solution was acidified with concentrated HCl (10 mL) and then evaporated to dryness on a hot water bath [33]. The reduced Schiff base ligand H_2L^R was extracted from the solid mass with methanol, and this methanol solution (ca. 25 mL, 5 mmol) was reacted with an aqueous solution (15 mL) of $\text{Ni}(\text{ClO}_4)_2\cdot 6\text{H}_2\text{O}$ (1.820 g, 5 mmol) and 10 mL of ammonia solution (20%) to prepare the “metalloligand”, $[\text{NiL}^R]$ as reported earlier [34].

2.3. Syntheses of the complexes, $[(\text{NiL}^R)_2\text{Fe}(\text{N}_3)_3]$ (**1**), $[(\text{NiL}^R(\text{H}_2\text{O}))_2\text{Fe}(\text{C}_6\text{H}_5\text{CH}_2\text{CO}_2)_2]\cdot(\text{HSO}_4)$ (**2**) and $[(\text{NiL}^R(\text{H}_2\text{O}))_2\text{Fe}(\text{C}_6\text{H}_5\text{CO}_2)_2]\cdot(\text{HSO}_4)\cdot(\text{H}_2\text{O})\cdot(\text{CH}_2\text{Cl}_2)$ (**3**)

The precursor complex $[\text{NiL}^R]$ (0.684 g, 2 mmol) was dissolved in methanol (20 mL) and then an aqueous solution (1 mL) of iron (III) sulphate (0.399 g, 1 mmol) and an aqueous solution (1 mL) of sodium azide (0.195 g, 3 mmol), were added to this solution. The mixture was stirred for 1 h and then filtered. The filtrate was allowed to stand overnight when deep red coloured micro-crystals of **1** appeared at the bottom of the beaker. Complexes **2** (red, rhombic) and **3** (red, hexagonal) were prepared using the same synthetic methods (and the same stoichiometries) as described for **1** but using sodium phenyl acetate (0.474 g, 3 mmol) and sodium benzoate (0.432 g, 3 mmol) respectively, instead of sodium azide. All three compounds were re-crystallised from dichloromethane solution to get X-ray quality single crystals. The crystals (**1–3**) were washed with a methanol–water mixture and dried in a desiccator containing anhydrous CaCl_2 and then characterized by elemental analysis, spectroscopic methods and X-ray diffraction.

Complex 1

Yield: 1.797 g, 51%. *Anal.* Calc. for $\text{C}_{136}\text{H}_{166}\text{Fe}_4\text{N}_{52}\text{Ni}_8\text{O}_{18}$: C, 46.52; H, 4.75; N, 20.67. Found: C, 46.38; H, 4.88; N, 20.82%; UV-Vis: λ_{max} in nm (solid, reflectance) = 490 and 349. IR (KBr) in cm^{-1} : $\nu(\text{N}-\text{H})$ 3254; $\nu(\text{N}_3)$ 2054.

Complex 2

Yield: 0.743 g, 64%. *Anal.* Calc. for $\text{C}_{50}\text{H}_{59}\text{FeN}_4\text{Ni}_2\text{O}_{15}\text{S}$: C, 51.71; H, 5.12; N, 4.82. Found: C, 51.76; H, 5.01; N, 4.89%; UV-Vis: λ_{max} in nm (solid, reflectance) = 510 and 352. IR (KBr) in cm^{-1} : $\nu(\text{N}-\text{H})$ 3261; $\nu(\text{C}=\text{O})$ 1569 and 1597.

Complex 3

Yield: 0.836 g, 69%. *Anal.* Calc. for $\text{C}_{49}\text{H}_{59}\text{FeN}_4\text{Ni}_2\text{O}_{15}\text{SCl}_2$: C, 48.23; H, 4.87; N, 4.59. Found: C, 48.41; H, 4.93; N, 4.71%; UV-Vis: λ_{max} in nm (solid, reflectance) = 492 and 350. IR (KBr) in cm^{-1} : $\nu(\text{N}-\text{H})$ 3257; $\nu(\text{C}=\text{O})$, 1553 and 1594.

2.4. Physical measurements

Elemental analyses (C, H, and N) were performed using a Perkin-Elmer 2400 series II CHN analyzer. IR spectra in KBr pellets (4000–400 cm^{-1}) were recorded using a Perkin-Elmer RXI FT-IR spectrophotometer. Electronic spectra in solid state (1200–300 nm) were recorded in a Hitachi U-3501 spectrophotometer. The DC magnetic susceptibility measurements were carried out in the temperature range 2–300 K with an applied magnetic field of 0.1 T on polycrystalline samples of compounds **1–3** (with masses of 30.48, 23.58 and 36.83 mg, respectively) with a Quantum Design MPMS-XL-5 SQUID susceptometer. AC susceptibility measurements were performed on compounds **2** and **3** in the temperature range 2–10 K with an oscillating field of 3.9 Oe at

110 Hz. The susceptibility data were corrected for the sample holders previously measured using the same conditions and for the diamagnetic contributions of the salt as deduced by using Pascal's constant tables ($\chi_{\text{dis}} = -529.6 \times 10^{-6}$, -531.6×10^{-6} and $-528.9 \times 10^{-6} \text{ emu mol}^{-1}$ respectively) [35].

2.5. Crystallographic data collection and refinement

Well formed single crystals of each complex was mounted on a Bruker-AXS SMART APEX II diffractometer equipped with a graphite monochromator and Mo K α ($\lambda = 0.71073 \text{ \AA}$) radiation. The crystals were positioned 60 mm from the CCD, and 360 frames were measured with a counting time of 5 s. The structures were solved using the Patterson method through the SHELXS 97 program. Non-hydrogen atoms were refined with independent anisotropic displacement parameters, while difference Fourier synthesis and least-squares refinement showed the positions of remaining non-hydrogen atoms. The hydrogen atoms bound to carbon atoms were included in geometric positions and given thermal parameters equivalent to 1.2 (or 1.5 for methyl groups) times those of the atom to which they were attached. Hydrogen atoms that bonded to N or O were located in a difference Fourier map where possible and refined with distance constraints. In **2** and **3**, the free anions were disordered and refined using distance constraints with 50% occupancy. Successful convergence was indicated by the maximum shift/error of 0.001 for the last cycle of the least-squares refinement. Absorption corrections were carried out using the SADABS program [36], while all calculations were made via SHELXS 97 [37], SHELXL 97 [38], PLATON 99 [39], ORTEP-32 [40], and WINGX system ver-1.64 [41]. Data collection, structure refinement parameters, and crystallographic data for the three complexes are given in Table S1.

3. Results and discussion

3.1. Syntheses of the complexes

The reduced Schiff-base ligand (H_2L^R) and its metalloligand, $[NiL^R]$ were synthesized using the reported procedures [32–34]. The “metalloligand”, $[NiL^R]$ on reaction with iron(III) sulphate and sodium azide or sodium phenyl acetate or sodium benzoate in 2:1:3 molar ratios in MeOH-H₂O medium (10:1, v/v) resulted in three new trinuclear Ni₂Fe complexes, $[(NiL^R)_2Fe(N_3)_3]$ (**1**) $[(NiL^R(H_2O))_2Fe(C_6H_5CH_2CO_2)_2] \cdot (HSO_4)$ (**2**) and $[(NiL^R(H_2O))_2Fe(C_6H_5CO_2)_2] \cdot (HSO_4) \cdot (H_2O) \cdot (CH_2Cl_2)$ (**3**) (Scheme 1).

3.2. IR and UV-Vis spectra

Besides elemental analyses, all three complexes were initially characterized by IR spectra. The appearance of moderately strong and sharp peaks at 3254, 3261 and 3257 cm⁻¹ (due to a N–H stretching vibration) for complexes **1–3**, respectively (Figs. S1–S3, S1) and absence of any peak at around 1620 cm⁻¹ indicate that the imine group of the Schiff base is reduced [17,18]. The peak at 2054 cm⁻¹ proves the presence of azido coligand for **1**. On the other hand, the presence of carboxylato ligand in complexes **2** and **3** is confirmed by the appearance of strong and sharp peaks at 1569 and 1553 cm⁻¹ along with shoulders at 1597 and 1594 cm⁻¹, respectively (Figs. S2 and S3, S1). The splitting of the band is indicative of the presence of two different types (symmetric and asymmetric) stretching vibrations of the carboxylato coligands.

The electronic spectra of the three compounds were recorded in the solid state (Fig. S4). Compounds **1–3** show broad absorption

bands at 490, 510 and 492 nm, respectively, while the band maxima for the “metalloligand” $[NiL^R]$ appear at 635 nm. These bands are attributed to d-d transitions of Ni(II) ions in octahedral environment. In addition, the three hetero-metallic compounds show a sharp single absorption maximum near 349, 352 and 350 nm for **1**, **2** and **3**, respectively, and the “metalloligand” $[NiL^R]$ shows an absorption maximum at 349 nm, attributed to ligand-to-metal charge transfer transitions.

3.3. Description of the structures

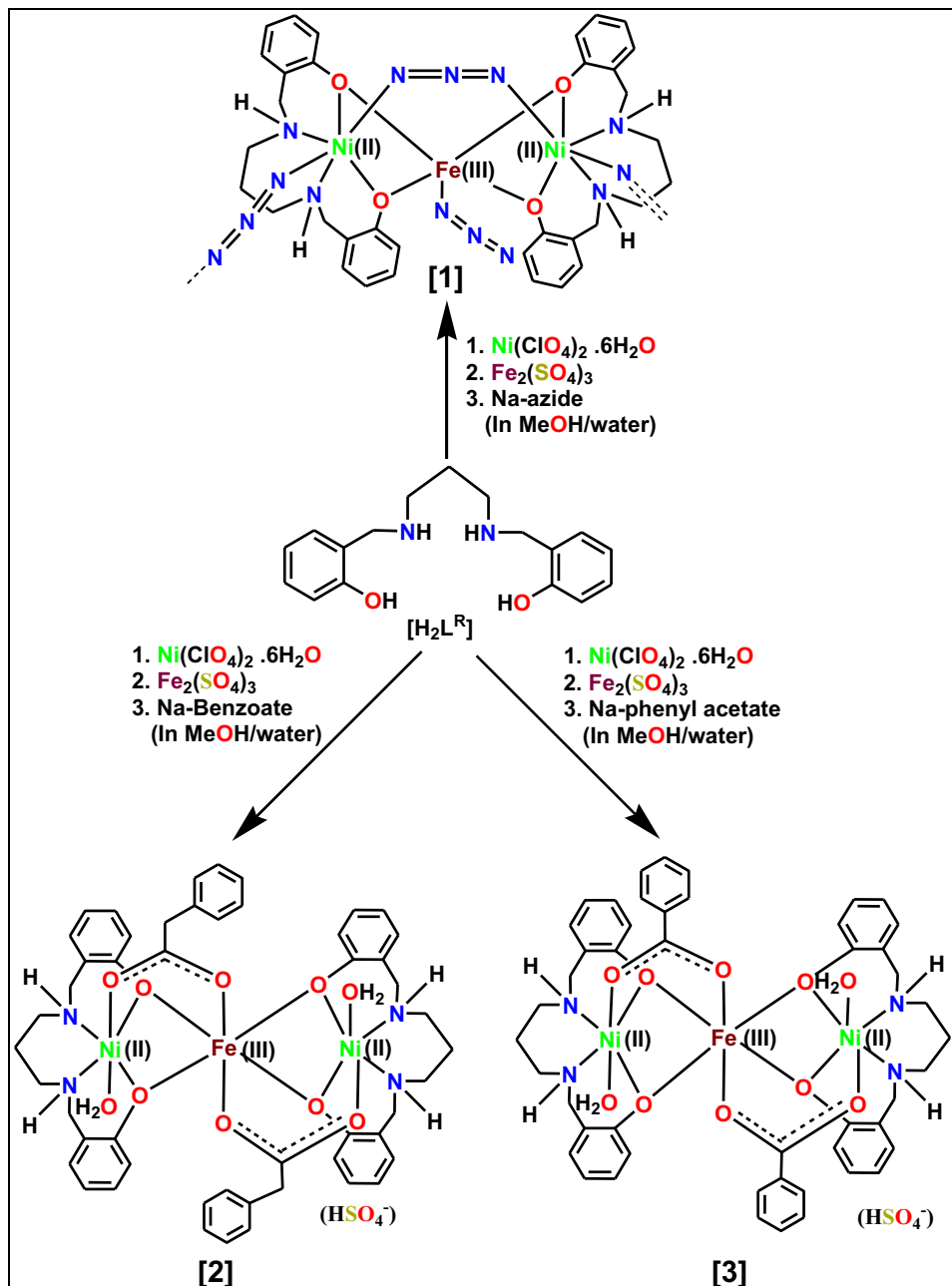
3.3.1. Complex **1**

The X-ray crystal structure shows that complex **1** is a $\mu_{1,3}\text{-N}_3$ bridged 1D chain (Fig. 1) based on trinuclear $[(NiL^R)_2Fe(N_3)_3]$ units.

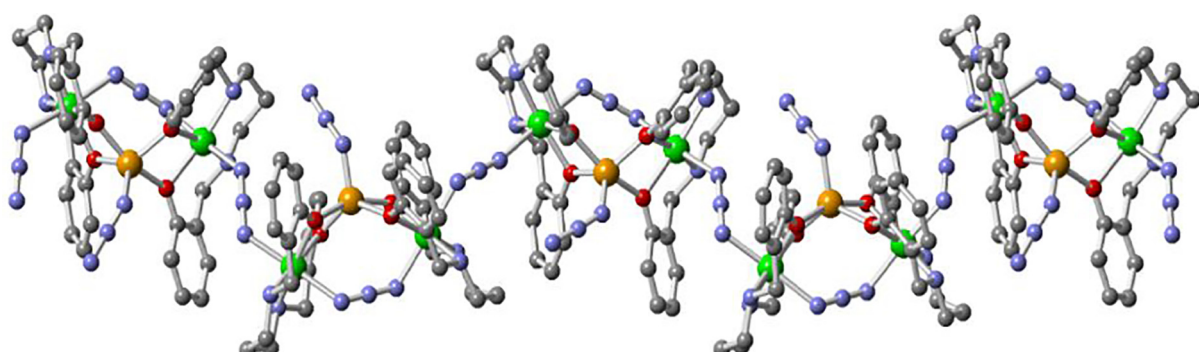
The asymmetric unit consists of four equivalent trinuclear $[(NiL^R)_2Fe(N_3)_3]$ units. The bond parameters are nearly the same in all four equivalent trinuclear structures; hence here we describe only one unit which is depicted in Fig. 2. Crystallographic data for this complex is given in Table S1. Selected bond lengths and angles are listed in Table S2. In each of the trinuclear units, the three metal atoms (two terminals Ni and one central Fe) are in a bent arrangement with $\angle Ni(\text{II})-\text{Fe}(\text{III})-Ni(\text{II})$ angles ranging from 109.4 (1) to 110.4(1) $^\circ$. The terminal nickel(II) atoms present a distorted octahedral geometry. The basal plane of the two terminal Ni(II) centers is formed by two μ_2 -phenoxido oxygen atoms and two imine nitrogen atoms of the chelated di-anionic tetradentate reduced Schiff-base ligand (L^R)²⁻ and the axial positions are occupied by two nitrogen atoms from two $\mu_{1,3}$ -bridging azido ligands. The four donor atoms in the equatorial plane around the nickel atoms show r.m.s. deviations between 0.01 and 0.05 Å in the eight independent coordination spheres while the nickel atoms deviate in the range 0.009(3) and 0.029(3) Å from the mean plane. The two equatorial planes intersect at 83.7(1)–88.1(1) $^\circ$ in the four trinuclear molecules. The Ni–O [2.039(4)–2.074(4) Å] and Ni–N [2.032(5)–2.072(5) Å] bond distances in the basal plane are very similar but these are shorter than the axial Ni–N bond distances [2.074(6)–2.168(6) Å] (Table S2). Both the bridging and terminal azido ligands are within 4° of being linear. The central Fe(1) atom is penta-coordinated by four phenoxido oxygen atoms of two reduced Schiff base ligands, and a terminal azido ligand. The distortions of the coordination geometry from the square pyramid to the trigonal bipyramidal have been calculated by the Addison parameter (τ) [42]. The value of τ is defined as the difference between the two largest donor-metal-donor angles divided by 60. The parameter τ is 0 for the ideal square pyramid and 1 for the trigonal bipyramidal. The τ values of the four Fe(1) ions range from 0.46 to 0.54, indicating that the geometry is intermediate between the two ideal geometries. The Fe–O bond distances [1.927(4)–2.024(4) Å] are larger than the Fe–N ones [1.900(6)–1.929(5) Å]. The metal–metal distances range between 3.074(1) and 3.120(1) Å.

3.3.2. Complexes **2** and **3**

The linear trinuclear structures of **2** and **3** having molecular formula $[(NiL^R(H_2O))_2Fe(C_6H_5CH_2CO_2)_2] \cdot (HSO_4)$ (**2**) and $[(NiL^R(H_2O))_2Fe(C_6H_5CO_2)_2] \cdot (HSO_4) \cdot (H_2O) \cdot (CH_2Cl_2)$ (**3**), respectively, are shown in Fig. 3 together with the atomic numbering scheme. The selected bond parameters are summarized in Table S3. Unlike **1**, both structures (**2** and **3**) contain a crystallographic inversion center at the central iron atom Fe(1). Thus, the asymmetric unit consists of two metal centers [Ni(II)-terminal and Fe(III)-central], one deprotonated reduced di-Schiff base ligand [(L^R) ²⁻], one bridging carboxylato co-anion (phenyl acetato for **2** and benzoato for **3**) and one non-coordinated hydrogen sulphate anion. These free anions are in general positions with 50% occupancy. In the case of **3** the



Scheme 1. Syntheses of complexes 1–3.

Fig. 1. The 1D chain of **1** formed by $\mu_{1,3}\text{-N}_3$ bridging between trinuclear units. Other H-atoms have been removed for clarity.

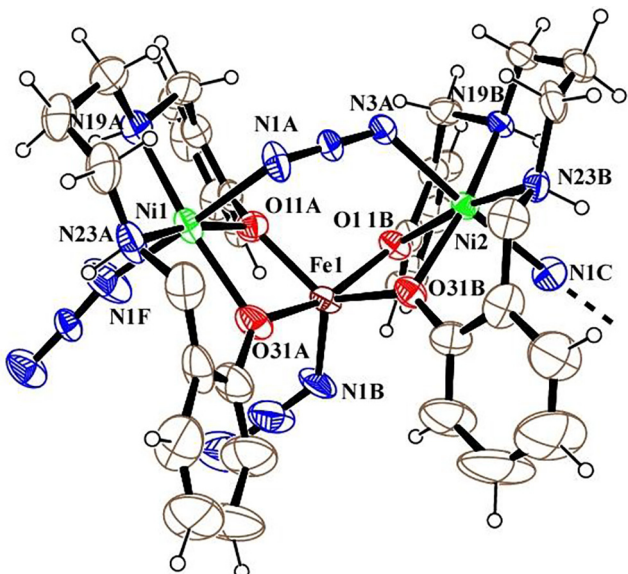


Fig. 2. Ortep structure of one trinuclear complex of **1** with ellipsoids at 30% probability. There are three other complexes with equivalent geometries in the asymmetric unit which together form a one-dimensional polymer. The solvent water molecules are omitted for clarity.

asymmetric unit contains a water and a dichloromethane molecule both refined with 50% occupancy. For charge balance the anions in **2** and **3** must be HSO_4^- though the hydrogen atom was not located. For both complexes, the terminal nickel center [Ni(1)] presents a distorted octahedral geometry. The basal plane of the Ni(1) in each case is formed by the two imine N atoms and two phenoxide oxygen atoms like **1** but unlike **1** the axial sites are occupied by the coordination of two O-atoms, one from a bridging carboxylato ligand and other from a water solvent molecule. All the bond distances Ni–N [2.061(5)–2.063(5) Å for **2** and 2.045(6)–2.079(6) Å for **3**] and Ni–O [2.058(4)–2.065(4) Å for **2** and 2.044(4)–2.053(4) Å for **3**] are very close to each other (Table S3), as in **1**. The range of *cis* angles [79.3(2)–96.8(2)° for **2** and 79.1(2)–96.3(3)° for **3**] and *trans* angles [170.9(2)–174.7(2)° for **2** and 170.8(3)–174.9(2)° for **3**] around the metal centres indicate that both coordination spheres deviate only slightly from the ideal

octahedral geometry. The distorted octahedral geometry of the nickel atoms in **2** and **3** is confirmed by the root mean squared (r.m.s.) deviations of the four basal atoms from the mean plane which are 0.008 and 0.012 Å with the metal atom 0.016(1) and 0.033(1) Å shifted from this mean plane, respectively.

For both structures (**2** and **3**), and in contrast to **1**, the central Fe(III) atom occupies a crystallographic inversion centre with a distorted octahedral geometry being bonded to four phenoxide oxygen atoms of deprotonated tetradeinate reduced Schiff base ligands and two oxygen atoms of two bridging carboxylato ligands. The basal Fe(III)–O bond distances [1.978(4)–1.980(4) Å for **2** and 1.970(4)–1.980(4) Å for **3**] are similar but shorter than the axial ones [2.044(4) and 2.041(4) Å for **2** and **3**, respectively] resulting in an axially elongated octahedron. The slight distortion of the octahedral geometry of Fe(III) is also indicated by the range of *cis* angles [83.3(2)–88.1(2)° for **2** and 82.6(2)–89.0(2)° for **3**]. The Fe(1)–Ni(1) distances are 3.029(1) and 3.012(1) Å for **2** and **3**, respectively.

Both structures (**2** and **3**) contain an intermolecular C–H··· π interaction between the centroid of phenyl ring of one unit and a H-atom of another similar unit with the dimensions C(21)–H(21B)–CG12, 144.1°; H(21B)–CG12, 2.88 Å; CG12 = C45–C46–C47–C48–C49–C50 for **2** and C(21)–H(21A)–CG12, 129.7°, H(21A)–CG12, 3.13 Å; CG12 = C44–C45–C46–C47–C48–C49 for **3** (Fig. 4 and Fig. S5, respectively). From the dimensions it is clear that this intermolecular C–H··· π interaction in **2** (Fig. 4) is stronger than that in **3** (Fig. S5).

In addition, both structures (**2** and **3**) also contain an intermolecular H-bonding interaction between the O atoms [O51 and O54 for **2**; O63 and O64 for **3**] of the non-coordinated hydrogen sulphate anion and the hydrogen atom (H19) of the reduced imine moiety [N(19)–H(19)···O(51)/O(54) and N(19)–H(19)···O(63)/O(64)] with the dimensions H19–O51/O54 2.37(5)/2.48(6) Å and H19–O63/O64 2.28(6)/2.39(9) Å; N(19)–H(19)···O(51)/O(54) 156(5)°/152(5)° and N(19)–H(19)···O(63)/O(64) 160(7)/150(4)° for **2** and **3**, respectively [Figs. S6 and S7].

3.4. Magnetic properties of the complexes

The thermal variation of the product of the molar magnetic susceptibility per Ni_2Fe trimer times the temperature ($\chi_m T$) for compound **1** shows a value of *ca.* 6.5 $\text{cm}^3 \text{K mol}^{-1}$ at room temperature, close to the expected value for two isolated Ni(II) ions

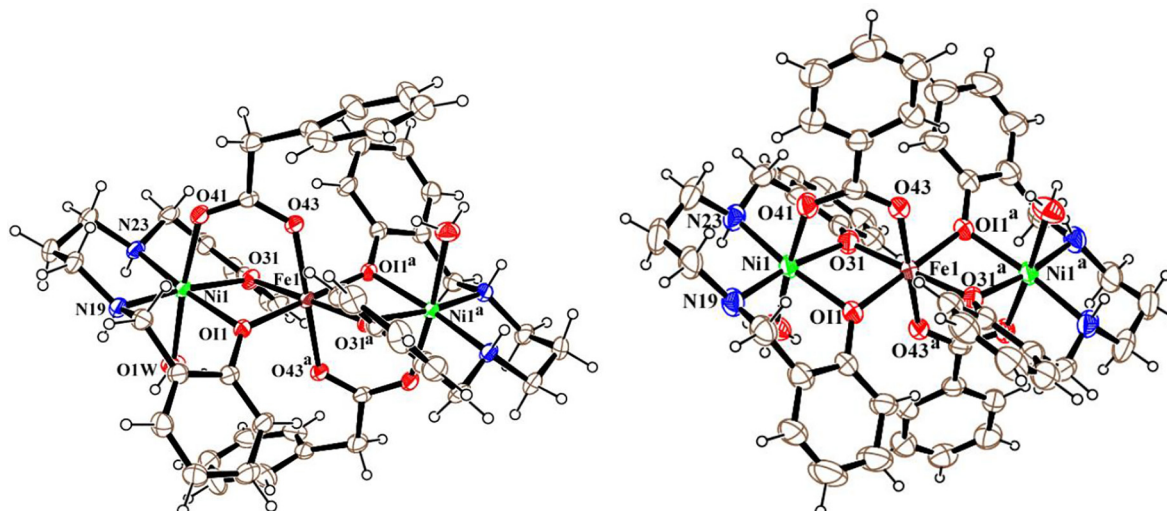


Fig. 3. Ortep structures of **2** (left) and **3** (right) with ellipsoids at 30% probability. Symmetry elements^a = 1 – x, 1 – y, 1 – z and 1/2 – x, 1/2 – y, 1 – z for **2** and **3**, respectively. Hydrogen sulphate anions in **2** and **3** are not shown for clarity nor are the solvent water molecules.

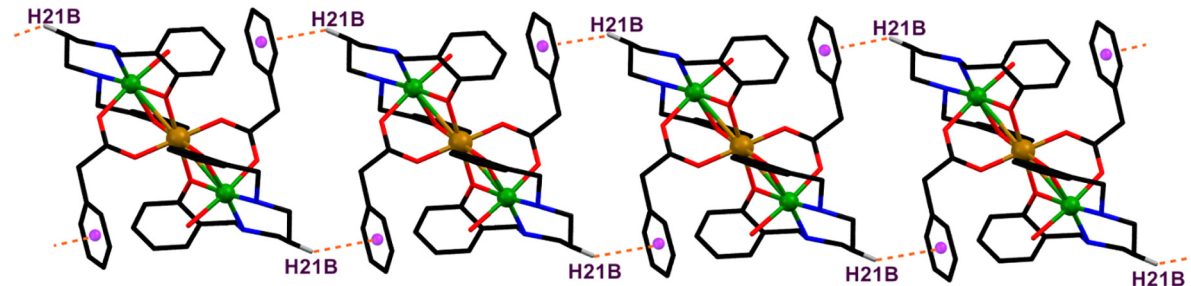


Fig. 4. The intermolecular C–H...π interaction between two trinuclear units in **2**. Other H-atoms have been removed for clarity.

(ca. $2 \text{ cm}^3 \text{ K mol}^{-1}$) plus one isolated Fe(III) ion (ca. $4.4 \text{ cm}^3 \text{ K mol}^{-1}$). When the temperature is lowered, $\chi_m T$ shows a progressive and continuous decrease to reach a small plateau of ca. $0.4 \text{ cm}^3 \text{ K mol}^{-1}$ in the range 3–5 K. Below ca. 3 K, $\chi_m T$ shows an additional decrease to reach a value of ca. $0.25 \text{ cm}^3 \text{ K mol}^{-1}$ at 2 K (Fig. 5). This behaviour suggests the presence of predominant antiferromagnetic Ni–Fe exchange interactions in compound **1**. The structure of compound **1** shows the presence of a chain of Ni_2Fe trimers connected through $\mu_{1,3}\text{-N}_3$ bridges. These Ni_2Fe trimers present two types of bridges: (i) double phenoxido bridges between $\text{Ni}(1)\text{-Fe}$ and $\text{Ni}(2)\text{-Fe}$ and (ii) a single $\mu_{1,3}\text{-N}_3$ bridge between the two Ni ions. Accordingly, we have fitted the magnetic properties of compound **1** with a chain of isosceles triangular trimers with three different coupling constants (J_1 and J_2 to account for the intra-trimer interactions and J_3 for the inter-trimer ones, see Fig. 6) [43,44]. This model reproduces very satisfactorily the magnetic properties of compound **1** above ca. 3 K with $g = 2.133$, $J_1 = -33.2 \text{ cm}^{-1}$, $J_2 = -19.9 \text{ cm}^{-1}$ and $J_3 = -16.7 \text{ cm}^{-1}$ (solid line in Fig. 5). Note that in order to reduce the number of adjustable parameters, we have assumed an average g value for the Ni(II) and Fe(III) ions.

The anti-ferromagnetic coupling found in the three exchange coupling constants in compound **1** can be rationalized from previous magneto-structural correlations in double oxido bridges (J_1) and in $\mu_{1,3}\text{-N}_3$ bridges (J_2 and J_3). Thus, the moderate anti-ferromagnetic coupling corresponding to J_1 (-33.2 cm^{-1}) agrees with the values found in the reported double phenoxido-bridged Fe–Ni complexes (Table 1). In **1** the Ni–O–Fe bond angles (in the range 98.4–102.3°) are above the crossing point (ca. 98°) between ferro- and anti-ferromagnetic coupling and, accordingly, the coupling is

anti-ferromagnetic [45–53]. On the other side, J_2 (-19.9 cm^{-1}) and J_3 (-16.7 cm^{-1}), correspond to $\mu_{1,3}\text{-N}_3$ bridges, which are well known to give rise to moderate-strong anti-ferromagnetic coupling when connecting transition metal ions [54–56]. Furthermore, for single $\mu_{1,3}\text{-N}_3$ bridges, the strength of this coupling strongly depends on the M–N–N angle (β) (that indicates the deviation from linearity of the $\mu_{1,3}\text{-N}_3$ bridge) in such a way that large β values imply large $|J|$ couplings [55]. This correlation agrees with our results since the average β angle in the $\mu_{1,3}\text{-N}_3$ bridge corresponding to J_2 ($\beta = 57.6^\circ$) is larger than the β angle in the $\mu_{1,3}\text{-N}_3$ bridge corresponding to J_3 ($\beta = 36.52^\circ$) and, accordingly, $|J_2|$ is larger than $|J_3|$. Additionally, the J_2 and J_3 values are close to those found in other Ni(II) complexes with single $\mu_{1,3}\text{-N}_3$ bridges and similar β angles [55].

The thermal variation of the product of the molar magnetic susceptibility per Ni_2Fe trimer times the temperature ($\chi_m T$) for compound **2** shows a room temperature value of ca. $6.7 \text{ cm}^3 \text{ K mol}^{-1}$, close to the expected value for two isolated Ni(II) ions (ca. $2.0 \text{ cm}^3 \text{ K mol}^{-1}$) plus a Fe(III) ion (ca. $4.4 \text{ cm}^3 \text{ K mol}^{-1}$) (Fig. 7). When the sample is cooled, the $\chi_m T$ product increases and reaches a maximum of ca. $8.2 \text{ cm}^3 \text{ K mol}^{-1}$ at ca. 8.2 K. Below this temperature $\chi_m T$ sharply decreases to reach a value of ca. $5.8 \text{ cm}^3 \text{ K mol}^{-1}$ at 2 K. This behaviour indicates the presence of predominant ferromagnetic Ni–Fe exchange interactions in the trimer whereas the sharp decrease at low temperatures has to be attributed to the zero field splitting (ZFS) of the resulting $S = 9/2$ ground spin state in the cluster. Since this cluster is a centro-symmetric linear trimer with no interactions between the terminal Ni centers (Fig. 7), we can fit the magnetic properties of compound **2** to a simple linear Ni–Fe–Ni trimer model with the symmetric magnetic scheme shown in Fig. 7 with only one coupling constant (J) and one average g value, using the hamiltonian: $H = -J(S_1S_2 + S_2S_3)$ with $S_1 = S_3 = 1$ and $S_2 = 5/2$ [43,44]. This model reproduces very satisfactorily the magnetic properties of compound **2** above the maximum with $g = 2.045$, $J = +4.9 \text{ cm}^{-1}$ and a 3.0% of paramagnetic contribution that may be due to the presence of defective clusters or monomeric species formed from the trimeric Ni_2Fe cluster (solid line in Fig. 7).

The weak ferromagnetic coupling found in compound **2** is the expected type given the Ni–O–Fe bond angles in compound **2** ($97.02(15)^\circ$ and $97.18(15)^\circ$) which are slightly below the crossing point (ca. 98°) between ferro and antiferromagnetic coupling for double oxido bridged metal complexes (Table 1) [45–53].

The thermal variation of the product of the molar magnetic susceptibility per Ni_2Fe trimer times the temperature ($\chi_m T$) for compound **3** is very similar to that of compound **2**: it shows a room temperature value of ca. $6.7 \text{ cm}^3 \text{ K mol}^{-1}$, as in **2**, and close to the expected value for two isolated Ni(II) ions and a Fe(III) one (Fig. 8). When cooling the sample $\chi_m T$ increases to reach a maximum of ca. $9.7 \text{ cm}^3 \text{ K mol}^{-1}$ at ca. 4.4 K. At lower temperatures $\chi_m T$ sharply decreases and reaches a value of ca. $8.3 \text{ cm}^3 \text{ K mol}^{-1}$ at 2 K. As for **2**, the increase in $\chi_m T$ indicates the presence of predominant ferromagnetic Ni–Fe exchange interactions in the trimer

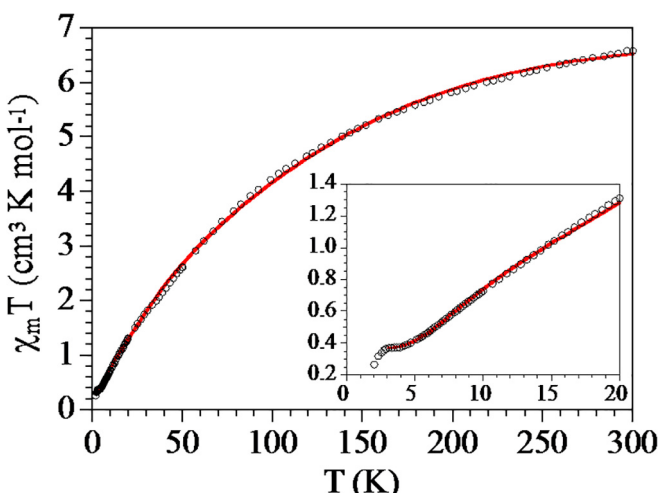


Fig. 5. Thermal variation of the $\chi_m T$ product per Ni_2Fe trimer for compound **1**. Solid line shows the fit to the model (see text). Inset shows the low temperature region.

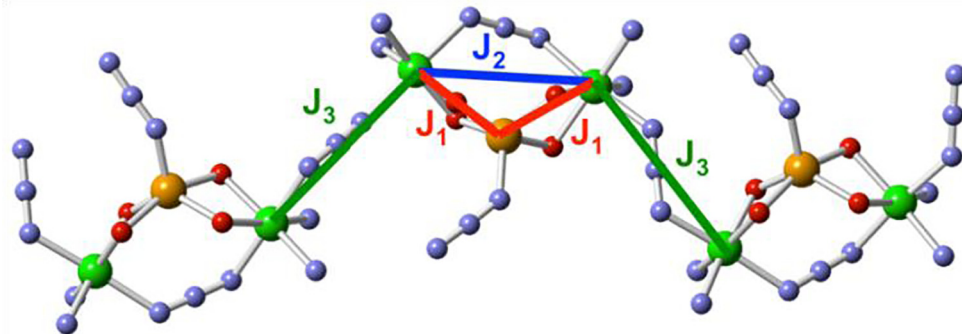


Fig. 6. View of the chain of Ni_2Fe triangles in **1** showing the magnetic exchange scheme used to fit the magnetic data.

Table 1

Selected structural parameters of previously reported phenoxido-bridged $\text{Ni}^{\text{II}}\text{--Fe}^{\text{III}}$ complexes and of compounds **1–3**.

Complexes ^a	$J_{\text{Ni}(\text{II})\text{--Fe}(\text{III})}$ (exptl)/cm ⁻¹	bridging moiety	Ni—O—Fe (°)	$\text{Ni}_2\text{O}_2\text{Fe}$ dihedral angle (°)	Refs.
1 [Fe ^{III} Ni ^{II} (IPCPMP)(OAc) ₂ (CH ₃ OH)][PF ₆] ₂	-33.2 -11.20	bis(μ_2 -phenoxido) (μ_2 -phenoxido) and bis(μ -acetato)	100.75 116.43	13.82 —	Present work [30b]
[Fe ^{III} (N ₃) ₂ (L ¹)Ni ^{II} (H ₂ O) ₂](ClO ₄) ₂	-9.22	bis(μ_2 -phenoxido)	99.70	0.02	[29b]
[Fe ^{III} (L ²)(BNPP)Ni ^{II} (H ₂ O) (μ -BNPP)][ClO ₄] ₂	-7.10	bis(μ -phenoxido) and μ -(bis(4-nitrophenyl)- phosphato)	98.79	8.14	[30a]
[Fe ^{III} (N ₃) ₂ (L ³)Ni ^{II} (H ₂ O) (CH ₃ CN)][ClO ₄] ₂	-3.14	bis(μ_2 -phenoxido)	97.33	0.93	[29c]
[Fe ^{III} (Ni ^{II} L ⁴) ₂]NO ₃ ·C ₂ H ₅ OH	-1.85	tris(μ_2 -phenoxido)	86.23	—	[31]
[Fe ^{III} (benzoato)L ¹]Ni ^{II} (H ₂ O) ($\mu_{1,3}$ -benzoato)][ClO ₄] ₂	0.50	bis(μ_2 -phenoxido) and μ -benzoato	95.24	8.73	[29b]
[Fe ^{III} (H ₂ O)L ⁵]Ni ^{II} (OAc) (μ -OAc)][ClO ₄]·2H ₂ O	1.7	bis(μ_2 -phenoxido) and μ -acetato	92.80	—	[29a]
3	3.0	bis(μ_2 -phenoxido) and μ -benzoato	97.00	16.16	Present work
2	4.9	bis(μ_2 -phenoxido) and μ -phenylacetato	97.10	13.96	Present work
[Fe ^{III} (benzoato)L ⁶]Ni ^{II} (H ₂ O) ($\mu_{1,3}$ -benzoato)][ClO ₄] ₂	5.65	bis(μ_2 -phenoxido) and μ -benzoato	93.35	7.04	[29b]
{[Fe ^{III} (OAc)(L ³)Ni ^{II} (H ₂ O) (μ -OAc)] _{0.6} ·[Fe ^{III} (L ³)Ni ^{II} (μ -OAc) ₂]·0.4}·(ClO ₄) ₂ ·1.1H ₂ O	7.36	bis(μ_2 -phenoxido) μ -acetato; bis(μ -phenoxido)bis(μ -acetato)	90.88	4.87	[29c]
[Fe ^{III} (L ⁶)Ni ^{II} (μ OAc) ₂] (ClO ₄) ₂ ·H ₂ O	13.00	bis(μ_2 -phenoxido) and μ -acetato	89.40	3.00	[29b]
[Fe ^{III} (L ⁶)Ni ^{II} (μ -OPr) ₂] (ClO ₄) ₂ ·H ₂ O	14.57	bis(μ -phenoxido)bis(μ -propionato)	88.67	2.63	[29b]

^a IPCPMP = 2-(N-isopropyl-N-((2-pyridyl)methyl)aminomethyl)-6-(N-(carboxymethyl)-N-((2-pyridyl)methyl)amino methyl)-4-methylphenol; H₂L¹ = [2+2] condensation products of 4-ethyl-2,6-diformylphenol and 1,3-diaminopropane; BNPP = bis(4-nitrophenyl)phosphate; H₂L² = tetraiminodiphenol macrocyclic ligand; H₂L³ = [2+2] condensation product of 4-methyl-2,6-diformylphenol and 2,2'-dimethyl-1,3-diaminopropane; H₃L⁴ = 1,1,1-tris(N-salicylideneaminomethyl)ethane; H₂L⁵ = tetraaminodiphenol macrocyclic ligand; H₂L⁶ = [2+2] condensation product of 4-ethyl-2,6-diformylphenol and 2,2-dimethyl-1,3-diaminopropane.

whereas the sharp decrease at low temperatures has to be attributed to the zero field splitting (ZFS) of the resulting $S = 9/2$ ground spin state in the cluster. Since the geometry of the cluster in **3** is identical to that of **2**, we have used the same trimeric model to fit the magnetic data [43,44]. This model reproduces very satisfactorily the magnetic properties of compound **3** above the maximum with $g = 2.044$, $J = +3.0 \text{ cm}^{-1}$ and a 1.2% of paramagnetic contribution that may be due to the presence of defective clusters or monomeric species formed from the trimeric Ni_2Fe cluster (solid line in Fig. 8).

As in **2**, the weak ferromagnetic coupling found in compound **3** is the expected type since the Ni—O—Fe bond angles in compound **3** ($96.93(18)^\circ$ and $97.07(17)^\circ$) are also slightly below the crossing point (*ca.* 98°) between ferro- and anti-ferromagnetic coupling for double oxido bridged metal complexes (Table 1) [45–53].

Finally, if we compare the isostructural clusters **2** and **3**, we should expect a slightly larger ferromagnetic coupling in **3** since the bridging Ni—O—Fe bond angles are slightly lower in **3** ($96.93(18)^\circ$ and $97.07(17)^\circ$), than in **2** ($97.02(15)^\circ$ and $97.18(15)^\circ$). The lower J value found in **3** ($+3.0 \text{ cm}^{-1}$ versus $+4.9 \text{ cm}^{-1}$ in **2**) may be due to the lower dihedral angle in the $\text{Ni}_2\text{O}_2\text{Fe}$ unit in complex **2** (159.56°) compared to complex **3** (161.82°).

None of these compounds (**2** and **3**) show an out of phase susceptibility in the temperature range 2–10 K, precluding the presence of a single molecule magnet behaviour or a slow relaxation process.

4. Conclusions

The reaction of the “metalloligand” $[\text{NiL}^R]$ (where, $\text{H}_2\text{L}^R = \text{N,N}'\text{-bis}(2\text{-hydroxybenzyl})\text{-1,3-propanediamine}$) with Fe^{III} in presence of azido or carboxylato ion has yielded three $\text{Ni}_2^{\text{II}}\text{Fe}^{\text{III}}$ complexes demonstrating that “metalloligand” synthetic approach is as effective for incorporating Fe^{III} as for other metal ions. In all three complexes, the central Fe^{III} ion is connected to two $[\text{NiL}^R]$ through double phenoxido bridges and they represent the second examples

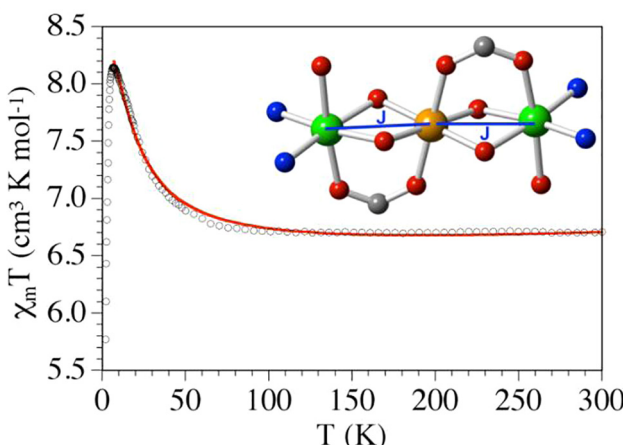


Fig. 7. Thermal variation of the $\chi_m T$ product per Ni_2Fe trimer for compound **2**. Solid line shows the best fit to the model (see text). Inset shows the linear Ni_2Fe complex in **2** with the magnetic exchange scheme used to fit the magnetic data (similar to **3**).

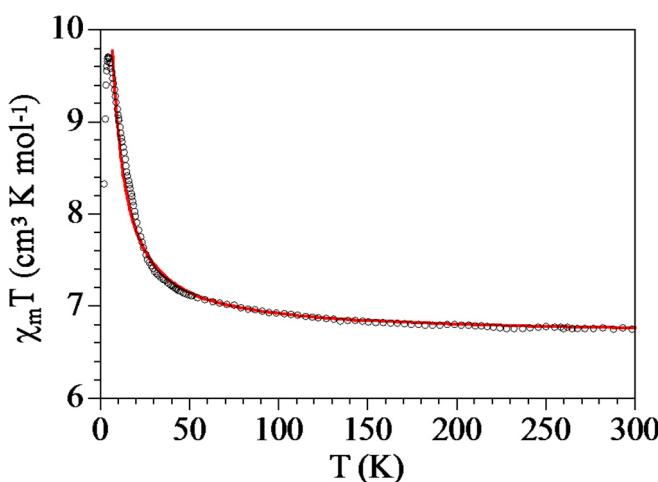


Fig. 8. Thermal variation of the $\chi_m T$ product per Ni_2Fe trimer for compound **3**. Solid line shows the best fit to the model (see text).

of such $\text{Ni}^{\text{II}}\text{Fe}^{\text{III}}$ species considering all kind of ligands and the first one with salen type reduced Schiff base ligands. Among the complexes, in **1**, the $\mu_{1,3}$ -azido bridge not only connects the terminal Ni^{II} centers within the trimer but it also joins the trinuclear units through $\text{Ni}(\text{II})$ to form a very rare type of chain for this type of ligand. On the other hand, in complexes **2** and **3**, the terminal Ni^{II} and central Fe^{III} are additionally bridged by carboxylato ions which is rather usual. In complex **1**, both the phenoxido bridges and $\mu_{1,3}$ -azido bridges mediate anti-ferromagnetic coupling, in good agreement with the magneto-structural correlations from the phenoxido bridging angles ($98.4\text{--}102.3^\circ$) and M–N–N angles (for azido). The phenoxido bridging angles in **2** and **3** are *ca.* 97° and the coupling is ferromagnetic which indicates that crossover angle is higher than 97° in these species. However, one should be cautious as the crossover angle can vary depending on other structural factors such as the dihedral angles in the central NiO_2Fe unit and the $\text{Ni}–\text{O}$ and $\text{Fe}–\text{O}$ bond distances.

Acknowledgements

The authors thank the Department of Science and Technology (DST – India), New Delhi, India, for financial support (SR/S1/IC/0034/2012). We also acknowledge the Generalitat Valenciana

– Spain (PrometeoII/2014/076 and ISIC Programs) for financial support.

Appendix A. Supplementary data

CCDC 1547125–1547127 contains the supplementary crystallographic data for (**1–3**). These data can be obtained free of charge via <http://www.ccdc.cam.ac.uk/conts/retrieving.html>, or from the Cambridge Crystallographic Data Centre, 12 Union Road, Cambridge CB2 1EZ, UK; fax: (+44) 1223-336-033; or e-mail: deposit@ccdc.cam.ac.uk. Supplementary data associated with this article can be found, in the online version, at <https://doi.org/10.1016/j.poly.2017.09.012>.

References

- [1] (a) D.S. Nesterov, O.V. Nesterova, V.N. Kokozay, A.J.L. Pombeiro, *Eur. J. Inorg. Chem.* (2014) 4496;
(b) E. Chelebaeva, J. Larionova, Y. Guari, R.A. SaFerreira, L.D. Carlos, F.A.A. Paz, A. Trifonov, C. Guérin, *Inorg. Chem.* 47 (2008) 775.
- [2] (a) M.L. Saha, X. Yan, P.J. Stang, *Acc. Chem. Res.* 49 (2016) 2527;
(b) P.G. Lacroix, I. Malfant, J.-A. Real, V. Rodriguez, *Eur. J. Inorg. Chem.* (2013) 615.
- [3] (a) C.N. Verani, E. Bothe, D. Burdinski, T. Weyhermüller, U. Flörke, P. Chaudhuri, *Eur. J. Inorg. Chem.* (2001) 2161;
(b) R. Biswas, Y. Ida, M.L. Baker, S. Biswas, P. Kar, H. Nojiri, T. Ishida, A. Ghosh, *Chem. Eur. J.* 19 (2013) 3943.
- [4] (a) E.I. Solomon, U.M. Sundaram, T.E. Machonkin, *Chem. Rev.* 96 (1996) 2563;
(b) J.I. van der Vlugt, *Eur. J. Inorg. Chem.* (2012) 363.
- [5] (a) S.J. Malthus, S.A. Cameron, S. Brooker, *Coord. Chem. Rev.* 316 (2016) 125;
(b) M. Atanasov, D. Aravena, E. Suturina, E. Bill, D. Maganas, F. Neese, *Coord. Chem. Rev.* 289 (2015) 177.
- [6] (a) F. Pointillart, Y. Le Gal, S. Golhen, O. Cador, L. Ouahab, *Inorg. Chem.* 47 (2008) 9730;
(b) F. Otte, P. Ferriani, S. Heinze, *Phys. Rev. B* 89 (2014) 205426 (1–19).
- [7] (a) V. Hoeke, A. Stammler, H. Bogge, J. Schnack, T. Glaser, *Inorg. Chem.* 53 (2014) 257;
(b) R.S. Evans, A.F. Schreiner, *Inorg. Chem.* 14 (1975) 1705.
- [8] (a) N.C. Martinez-Gomez, H.N. Vu, E. Skovran, *Inorg. Chem.* 55 (2016) 10083;
(b) C. Cruz, E. Spodine, A. Vega, D. Venegas-Yazigi, V. Paredes-Garcia, *Cryst. Growth. Des.* 16 (2016) 2173.
- [9] (a) L. Chatelain, J.P.S. Walsh, J. Pecaut, F. Tuna, M. Mazzanti, *Angew. Chem. Int. Ed.* 53 (2014) 13434;
(b) S.G. Minasian, J.L. Krinsky, J.D. Rinehart, R. Coping, T. Tyliszczak, M. Janousch, D.K. Shuh, J. Arnold, *J. Am. Chem. Soc.* 131 (2009) 13767;
(c) S.A. Kozimor, B.M. Bartlett, J.D. Rinehart, J.R. Long, *J. Am. Chem. Soc.* 129 (2007) 10672.
- [10] (a) F. Walz, E. Moos, D. Garnier, R. Köppé, C.E. Anson, F. Breher, *Chem. Eur. J.* 23 (2017) 1173;
(b) L.-Q. Chai, L.-J. Tang, L.-C. Chen, J.-J. Huang, *Polyhedron* 122 (2017) 228.
- [11] (a) C. Benelli, D. Gatteschi, *Chem. Rev.* 102 (2002) 2369;
(b) M. Andruh, J.P. Costes, C. Diaz, S. Gao, *Inorg. Chem.* 48 (2009) 3342.
- [12] (a) M. Maity, M.C. Majee, S. Kundu, S.K. Samanta, E.C. Sanudo, S. Ghosh, M. Chaudhury, *Inorg. Chem.* 54 (2015) 9715;
(b) F. Evangelisti, R. More, F. Hodel, S. Luber, G.R. Patzke, *J. Am. Chem. Soc.* 137 (2015) 11076;
(c) S. Ghosh, S. Biswas, A. Bauzá, M. Barceló-Olivier, A. Frontera, A. Ghosh, *Inorg. Chem.* 52 (2013) 7508.
- [13] (a) L.K. Das, A. Biswas, A. Frontera, A. Ghosh, *Polyhedron* 52 (2013) 1416;
(b) A. Hazari, L.K. Das, A. Bauzá, A. Frontera, A. Ghosh, *Dalton Trans.* 45 (2016) 5730.
- [14] C. Chen, D. Huang, X. Zhang, F. Chen, H. Zhu, Q. Liu, C. Zhang, D. Liao, L. Li, L. Sun, *Inorg. Chem.* 42 (2003) 3540.
- [15] (a) S. Ghosh, S. Giri, A. Ghosh, *Polyhedron* 102 (2015) 366;
(b) A. Hazari, A. Ghosh, *Polyhedron* 87 (2015) 403;
- [16] (c) L.K. Das, A. Ghosh, *CrystEngComm* 15 (2013) 9444.
- [17] (a) L.K. Das, M.G.B. Drew, A. Ghosh, *Inorg. Chim. Acta* 394 (2013) 247;
(b) S. Ghosh, S. Mukherjee, P. Seth, P.S. Mukherjee, A. Ghosh, *Dalton Trans.* 42 (2013) 13554.
- [18] (a) A. Hazari, L.K. Das, A. Bauzá, A. Frontera, A. Ghosh, *Dalton Trans.* 43 (2014) 8007;
(b) A. Hazari, S. Giri, C. Diaz, A. Ghosh, *Polyhedron* 118 (2016) 70.
- [19] (c) A. Hazari, L.K. Das, R.M. Kadam, A. Bauzá, A. Frontera, A. Ghosh, *Dalton Trans.* 44 (2015) 3862;
(b) A. Hazari, A. Das, P. Mahapatra, A. Ghosh, *Polyhedron* 134 (2017) 99.
- [20] (a) P. Bhowmik, S. Jana, P. Jana, K. Harms, S. Chattopadhyay, *Inorg. Chem. Commun.* 18 (2012) 50;
(b) Z.-L. You, Y. Lu, N. Zhang, B.-W. Ding, H. Sun, P. Hou, C. Wang, *Polyhedron* 30 (2011) 2186;
(c) G.A. Brewer, E. Sinn, *Inorg. Chem.* 26 (1987) 1529.

- [20] (a) F. Ercan, D. Ulku, O. Atakol, F.N. Dincer, *Acta Crystallogr., Sect. C: Cryst. Struct. Commun.* 54 (1998) 1787;
 (b) C. Fukuhara, K. Tsuneyoshi, N. Matsumoto, S. Kida, M. Mikuriya, M. Mori, J. Chem. Soc., Dalton Trans. (1990) 3473.
- [21] (a) L.K. Das, C.J. Gómez-García, M.G.B. Drew, A. Ghosh, *Polyhedron* 87 (2015) 311;
 (b) H. Oshio, M. Nihei, S. Koizumi, T. Shiga, H. Nojiri, M. Nakano, N. Shirakawa, M. Akatsu, J. Am. Chem. Soc. 127 (2005) 4568;
 (c) C.N. Verani, E. Rentschler, T. Weyhermüller, E. Bill, P. Chaudhuri, J. Chem. Soc., Dalton Trans. (2000) 251.
- [22] (a) L.K. Das, R.M. Kadam, A. Bauzá, A. Frontera, A. Ghosh, *Inorg. Chem.* 51 (2012) 12407;
 (b) S. Ghosh, G. Aromí, P. Gamez, A. Ghosh, *Eur. J. Inorg. Chem.* (2015) 3028.
- [23] (a) P. Seth, A. Figuerola, J. Jover, E. Ruiz, A. Ghosh, *Inorg. Chem.* 53 (2014) 9296;
 (b) L.K. Das, A. Biswas, C.J. Gómez-García, M.G.B. Drew, A. Ghosh, *Inorg. Chem.* 53 (2014) 434;
 (c) F. Ercan, M.B. Ates, Y. Ercan, S. Durmus, O. Atakol, *Cryst. Res. Technol.* 39 (2004) 470.
- [24] G.A. Brewer, E. Sinn, *Inorg. Chim. Acta* 134 (1987) 13.
- [25] I. Morgenstern-Badarau, D. Laroque, E. Bill, H. Winkler, A.X. Trautwein, F. Robert, Y. Jeannin, *Inorg. Chem.* 30 (1991) 3180.
- [26] T. Kobayashi, T. Yamaguchi, H. Ohta, Y. Sunatsuki, M. Kojima, N. Re, M. Nonoyama, N. Matsumoto, *Chem. Commun.* (2006) 1950.
- [27] P. Seth, A. Figuerola, J. Jover, E. Ruiz, A. Ghosh, *Polyhedron* 117 (2016) 57.
- [28] (a) Z. Lu, M. Yuan, F. Pan, S. Gao, D. Zhang, D. Zhu, *Inorg. Chem.* 45 (2006) 3538;
 (b) R. Biswas, P. Kar, Y. Song, A. Ghosh, *Dalton Trans.* 40 (2011) 5324;
 (c) D.V. Yazigia, D. Aravenab, E. Spodineb, E. Ruiz, S. Alvarez, *Coord. Chem. Rev.* 254 (2010) 2086.
- [29] (a) S.K. Dutta, R. Werner, U. Florke, S. Mohanta, K.K. Nanda, W. Haase, K. Nag, *Inorg. Chem.* 35 (1996) 2292;
 (b) S. Sasmal, S. Roy, L. Carrella, A. Jana, E. Rentschler, S. Mohanta, *Eur. J. Inorg. Chem.* (2015) 680;
 (c) S. Hazra, S. Bhattacharya, M.K. Singh, L. Carrella, E. Rentschler, T. Weyhermüller, G. Rajaraman, S. Mohanta, *Inorg. Chem.* 52 (2013) 12881.
- [30] (a) S. Dutta, P. Biswas, *Polyhedron* 31 (2012) 110;
 (b) M. Jarenmark, M. Haukka, S. Demeshko, F. Tuczek, L. Zuppiroli, F. Meyer, E. Nordlander, *Inorg. Chem.* 50 (2011) 3866;
 T.R. Holman, C. Juarez-Garcia, M.P. Hendrich, L. Jr, E. Munck Que, J. Am. Chem. Soc. 112 (1990) 7611.
- [31] S.C. Batista, A. Neves, A.J. Bortoluzzi, I. Vencato, R.A. Peralta, B. Szpoganicz, V.V. E. Aires, H. Terenzi, P.C. Severino, *Inorg. Chem. Commun.* 6 (2003) 1161.
- [32] L.K. Das, S.-W. Park, S.J. Cho, A. Ghosh, *Dalton Trans.* 41 (2012) 11009.
- [33] (a) A. Biswas, M.G.B. Drew, A. Ghosh, *Polyhedron* 29 (2010) 1029;
 (b) G.J.B. Colpas, J. Hamstra, J.W. Kampf, V.L. Pecoraro, *Inorg. Chem.* 33 (1994) 4669.
- [34] O. Atakol, H. Nazir, C. Arici, S. Durmus, I. Svoboda, H. Fuess, *Inorg. Chim. Acta* 342 (2003) 295.
- [35] G.A. Bain, J.F. Berry, *J. Chem. Educ.* 85 (2008) 532.
- [36] SAINT, version 6.02; SADABS, version 2.03, Bruker AXS Inc, Madison, WI, (2002).
- [37] G.M. Sheldrick, *SHELXS 97*, University of Göttingen, Germany, Program for Structure Solution, 1997.
- [38] G.M. Sheldrick, *SHELXL 97*, University of Göttingen, Germany, Program for Crystal Structure Refinement, 1997.
- [39] A.L. Spek, *J. Appl. Crystallogr.* 36 (2003) 7.
- [40] L.J.J. Farrugia, *J. Appl. Crystallogr.* 30 (1997) 565.
- [41] L.J.J. Farrugia, *J. Appl. Crystallogr.* 32 (1999) 837.
- [42] A.W. Addison, T.N. Rao, J. Reedijk, J.V. Rijn, G.C. Verschoor, *J. Chem. Soc., Dalton Trans.* (1984) 1349.
- [43] J.J. Borrás-Almenar, J.M. Clemente-Juan, E. Coronado, B.S. Tsukerblat, *Inorg. Chem.* 38 (1999) 6081.
- [44] J.J. Borrás-Almenar, J.M. Clemente-Juan, E. Coronado, B.S. Tsukerblat, *J. Comput. Chem.* 22 (2001) 985.
- [45] M.A. Halcrow, J. Sun, J.C. Huffman, G. Christou, *Inorg. Chem.* 34 (1995) 4167.
- [46] J.M. Clemente-Juan, B. Chansou, B. Donnadieu, J. Tuchagues, *Inorg. Chem.* 39 (2000) 5515.
- [47] L.K. Das, C.J. Gómez-García, A. Ghosh, *Dalton Trans.* 44 (2015) 1292.
- [48] J.M. Clemente-Juan, E. Coronado, J.R. Galán-Mascarós, C.J. Gómez-García, *Inorg. Chem.* 38 (1999) 55.
- [49] C.J. Gómez-García, E. Coronado, L. Ouahab, *Angew. Chem. Int. Ed.* 31 (1992) 649.
- [50] C.J. Gómez-García, J.J. Borrás-Almenar, E. Coronado, L. Ouahab, *Inorg. Chem.* 33 (1994) 4016.
- [51] S. Shit, M. Nandy, G. Rosair, C.J. Gómez-García, J.J.B. Almenar, S. Mitra, *Polyhedron* 61 (2013) 73.
- [52] A.K. Sharma, F. Lloret, R. Mukherjee, *Inorg. Chem.* 52 (2013) 4825.
- [53] A.K. Sharma, F. Lloret, R. Mukherjee, *Inorg. Chem.* 46 (2007) 5128.
- [54] Y. Zeng, X. Hu, F. Liu, X. Bu, *Chem. Soc. Rev.* 38 (2009) 469.
- [55] F.F. De Biani, E. Ruiz, J. Cano, J.J. Novoa, S. Alvarez, *Inorg. Chem.* 39 (2000) 3221.
- [56] J. Ribas, A. Escuer, M. Monfort, R. Vicente, R. Cortés, L. Lezama, T. Rojo, *Coord. Chem. Rev.* 193–195 (1999) 1027.